

# P5.14 THE SENSITIVITY OF WRF SIMULATIONS OF HURRICANE IVAN TO CHOICE OF CUMULUS PARAMETERIZATION

Megan S. Gentry<sup>+</sup> and Gary M. Lackmann  
*North Carolina State University*

## 1. INTRODUCTION

As progressively smaller grid spacing is used in numerical modeling of mesoscale weather systems, explicit simulation of convection without parameterization has become more common. However, to our knowledge, the appropriateness of omitting the cumulus parameterization (CP) scheme at smaller grid spacing (4 km or less) has not been systematically determined in a *tropical* environment, particularly for tropical cyclones. The objective of this study is to observe the effects of explicitly resolving convection in a tropical cyclone, as opposed to using a convective parameterization. It is our hypothesis that explicit treatment of convection will provide a more realistic representation of the hurricane secondary circulation, eye and eyewall structure, and storm intensity.

## 2. BACKGROUND

The use of different convective parameterizations and of explicitly resolved convection significantly impacts the simulated track and intensity of tropical cyclones (e.g., Davis and Bosart 2002). Even the choice of CP used on coarser, outer grids affects the explicitly resolved convection on the finer-mesh grids for which they provide lateral boundary conditions. In their three-domain case study of summer convection in the southwestern U.S., Warner and Hsu (2000) concluded that mass field adjustments on the outer grids affect the timing and intensity of precipitation in the innermost finer grid, producing up to a factor of 3 difference in the 24-hour explicit precipitation totals. They proposed possible ways of mitigating this problem which included testing “the adequacy of marginal grid resolutions (3-5 km) for the explicit simulation of convection.”

Weisman et al. (1997) simulated squall lines to test the sensitivity of horizontal grid resolution on explicit convection, using grid spacings between 1 and 12 km. This study concluded that 4 km grid spacing could reproduce essential features of the structure and evolution of the squall line seen in a 1 km run. Weisman et al. (1997, p. 546) speculate that this minimal resolution may be smaller in tropical environments in order to resolve the weaker vertical motions found in tropical cyclones relative to that found in intense midlatitude convective systems. Bryan et al. (2003) recommend grid spacings on the order of 100 m to be used as a benchmark in resolution sensitivity studies in order to better represent intracloud motions.

## 3. METHODS

The Weather Research and Forecasting (WRF) model (Version 2.0.3.1) is used for five different forecasts, all of which used the same physics and grid specifications, except for the CP scheme. In all of the simulations, a one-way nested grid of three domains is used, with 27, 9, and 3 km grid spacing on the outermost to innermost domains, respectively (Fig. 1).

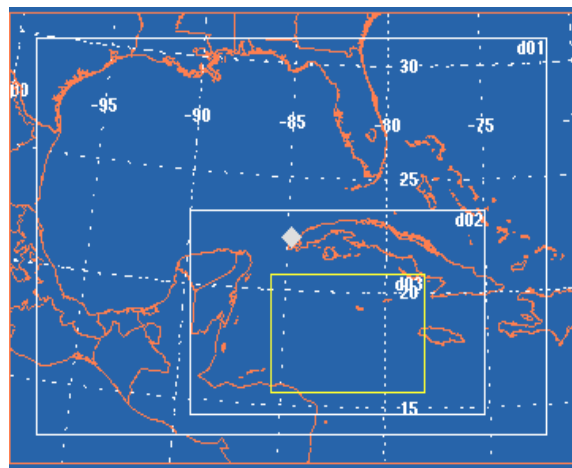


Fig. 1. Domain configuration used with grid spacing of 27, 9, and 3 km on domains 1, 2, and 3, respectively.

<sup>+</sup> Corresponding author address: Megan Gentry, North Carolina State University, Department of Marine, Earth and Atmospheric Sciences, Raleigh, NC 27695-8208. E-mail: msgentry@ncsu.edu

The WSM 6-class graupel microphysics parameterization and the Mellor-Yamada-Janjic (Janjic 1994) planetary boundary layer scheme are used on all domains for all forecasts. All domains are initialized on 11 September 2004 at 0000 UTC using Global Forecast System (GFS) initial conditions and 0.5 degree Real-Time Global sea-surface temperature analysis (Thiebaut et al. 2003). Lateral boundary conditions are provided by the GFS forecasts from the same forecast cycle as for the initial conditions. The Betts-Miller-Janjic (BMJ; Betts and Miller 1993) and Kain-Fritsch (KF; Kain and Fritsch 1993) CP schemes are turned on and off in the 3 km innermost grid, as described in table 1, with all grid dimensions and other physics options held constant. An additional simulation is run without a CP scheme on any of the 3 domains.

In order to more clearly isolate differences arising from CP choices in cross-sectional format through Ivan, a subset of model output variables is radially averaged. This is accomplished by averaging all points within 300 km of the storm center, which is defined as the local minimum of sea-level pressure, in concentric rings of 3 km width. Radial bins that are under-sampled, where less than five points were included in the average, were replaced with missing values. However, averages at farther distances will have more points sampled since the circumference around the storm center is greater at larger distances.

These radially averaged variables are then temporally averaged from forecast hours 24 to 48. Times before and after this period are excluded in order to prevent lateral boundary effects from influencing the signal. This process also enables difference fields to be computed in a storm-relative sense for each simulation after radial averaging is performed.

#### 4. HURRICANE IVAN OVERVIEW

Hurricane Ivan was one of the more notable storms of the 2004 season, intensifying to a category 5 storm on three separate occasions. After moving off the western African coast, Ivan reached hurricane status on 5 September, while still slightly south of 10°N latitude, and continued moving westward before taking a northwestward turn.

Designation	Cumulus Parameterization Scheme		
	Domain 1	Domain 2	Domain 3
00	explicit	explicit	explicit
B0	BMJ	BMJ	explicit
BB	BMJ	BMJ	BMJ
K0	KF	KF	explicit
KK	KF	KF	KF

Table 1. Designations used for different CP configurations on the coarser to finer grids, domains 1 to 3, respectively.

Hurricane Ivan reached its lowest minimum central pressure of 910 hPa on both 12 and 13 September, while passing west of Jamaica and the western tip of Cuba, and weakened to a category 3 storm before its landfall just west of Gulf Shores, Alabama on 16 September. Ivan then merged with a frontal system and transitioned to an extratropical low two days later. However, a remnant of Ivan tracked down the east coast in a large anticyclonic loop, re-emerging as a tropical depression and making its second U.S. landfall as a tropical depression in southwestern Louisiana on 24 September (Stewart 2004).

## 5. DISCUSSION

Significant differences in the hurricane structure and intensity on the innermost domain are found between all five runs, although this study will focus on runs with CP on the outermost grids. The inner domain is relatively small in comparison to the distance traversed by Ivan, so the tracks produced by the different runs are similar. Therefore, this study will focus mainly on comparing the structural differences seen in the runs where the BMJ and KF parameterizations are systematically turned on and off on the 3-km grid to test sensitivity.

### 5.1 Intensity

Intensity varies by as much as 28 hPa between the five runs, with 00 consistently weaker than the other simulations (Fig. 2). A minimum central pressure of 919 hPa in the B0 simulation is the lowest realized in any run. This run also exhibits the most favorable comparison with National Hurricane Center best track for sea level pressure. Simulation BB is slightly weaker, with a minimum central pressure of 926 hPa.

Simulations K0 and KK had lowest minimum central pressures of 937 and 942 hPa, respectively. The 00 simulation deepened the hurricane the least, with a minimum central pressure of 947 hPa.

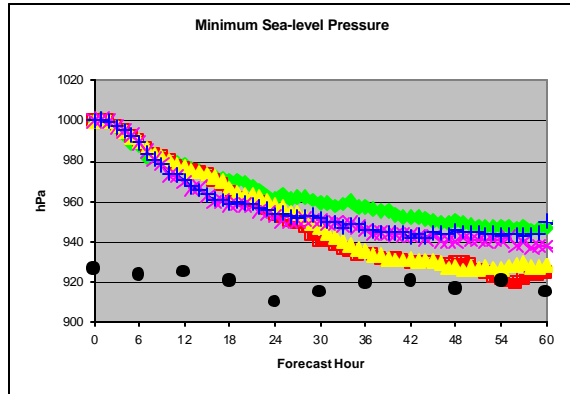


Fig. 2. Minimum central pressure as a function of time for 00 (green), B0 (red), BB (yellow), K0 (purple), and KK (blue), plotted with best track observations (black) from the National Hurricane Center.

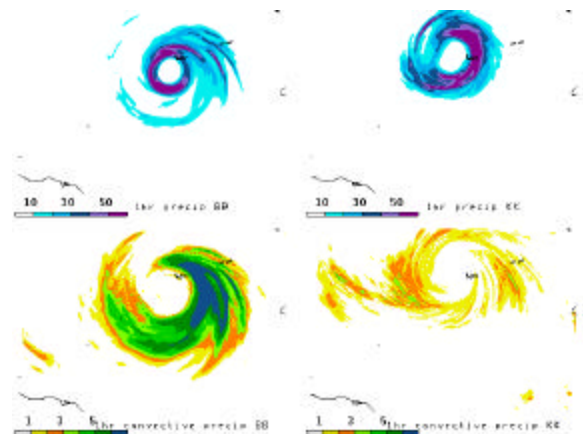


Fig. 3. Total hourly precipitation ending at forecast hour 36 for BB (top left), KK (top right), shaded every 10 mmhr<sup>-1</sup>. Hourly convective precipitation for BB (bottom left), and KK (bottom right), shaded every 1 mmhr<sup>-1</sup>.

### 5.2 CP Scheme Activity

The significance of this comparison between the simulations with no CP to those with schemes is best realized if the CP scheme is active in the KK and BB runs. The BMJ scheme produced more precipitation on the 3km grid than did the KF scheme, although the precipitation from the CP

scheme in both of these runs is approximately 10% of the total precipitation (Fig 3).

### 5.3 Simulated Radar

With explicit convection on the inner domain, the model-simulated radar exhibits a discontinuous, ragged eyewall with numerous, larger reflectivity cores of convection in the spiral bands relative to runs employing a CP scheme (Fig. 4).

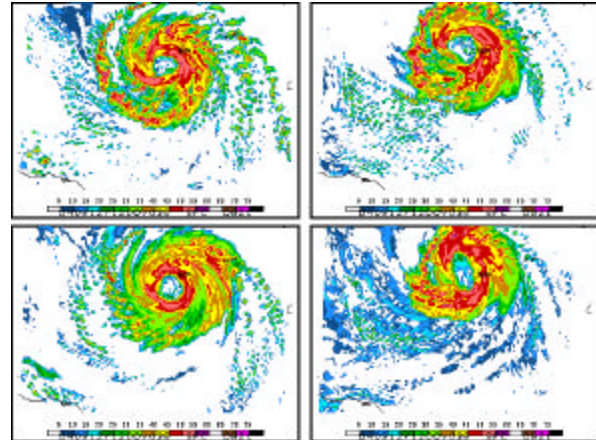


Fig. 4. Simulated radar reflectivity during forecast hour 36 for B0 (top left), BB (bottom left), K0 (top right), and KK (bottom right).

This difference is more noticeable between the BMJ runs than between the KF simulations, and can be more clearly seen with animated radar imagery. This is consistent with less KF activity relative to BMJ activity as seen in Fig. 3.

### 5.4 Vertical Motions

The vertical motions in these simulations are examined using radially averaged cross-sections, as described in section 4. The B0 simulation has the strongest and most concentrated eyewall updrafts of any simulation, with areas of average ascent above 1.5 ms<sup>-1</sup> leaning outwards with height from the warm core eye (Fig. 5a).

Comparison between the K0 and KK runs also follows the same trend seen in the BMJ runs, with the explicit simulation having an area of stronger, more concentrated updrafts in the eyewall. However, the magnitude of the updrafts in K0 is smaller, yielding a smaller difference between the KF simulations (not shown).

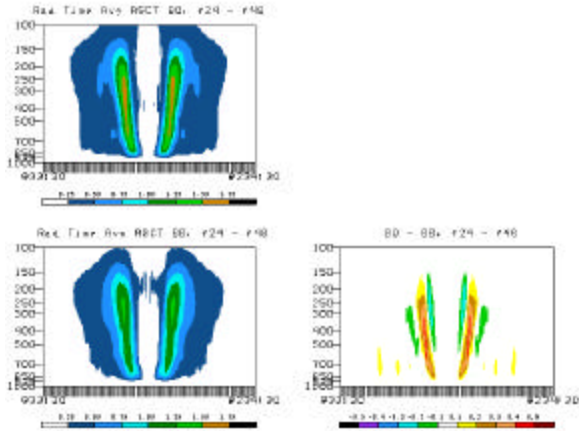


Fig. 5. Radial and time averaged cross-sections of ascent ( $\text{ms}^{-1}$ ) for B0 (top left), BB (bottom left) shaded every  $0.25 \text{ ms}^{-1}$ , and the difference field (bottom right) with BB subtracted from B0 shaded every  $0.1 \text{ ms}^{-1}$ . Warmer colors denote where B0 is greater than BB, with cooler colors shaded where BB is greater.

In order to avoid cancellation, a separate comparison is made for the average downward vertical velocity (Fig. 6). This comparison reveals a similar trend as evident for upward motions, with the explicit simulations producing stronger subsidence both in the eye and eyewall and at especially at lower altitudes within the eyewall (Fig. 6). These downdrafts presumably represent a response to grid-scale precipitation processes, such as evaporational cooling.

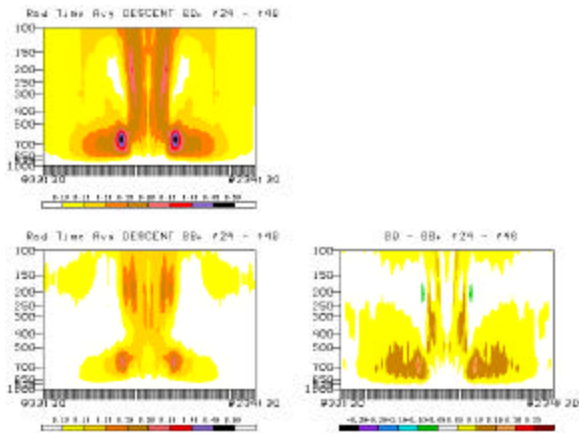


Fig. 6. As above with average descent ( $\text{ms}^{-1}$ ) for B0 (top left), BB (bottom left), and the difference field (bottom right) with BB subtracted from B0. All fields are shaded every  $0.05 \text{ ms}^{-1}$ , with color shading as above.

The B0 simulation produces strong cores of descent greater than  $0.45 \text{ ms}^{-1}$  in the lower eyewall, with a broad area of greater than  $0.25 \text{ ms}^{-1}$  of subsidence inside the eyewall. Again, this signal is clearer in comparing the two BMJ runs,

with the KF simulations being more similar to each other (not shown).

The K0 run has the most intense, concentrated area of subsidence inside the eyewall. However, B0 had stronger downdrafts in the lower levels of the eyewall than any other run (Fig. 7).

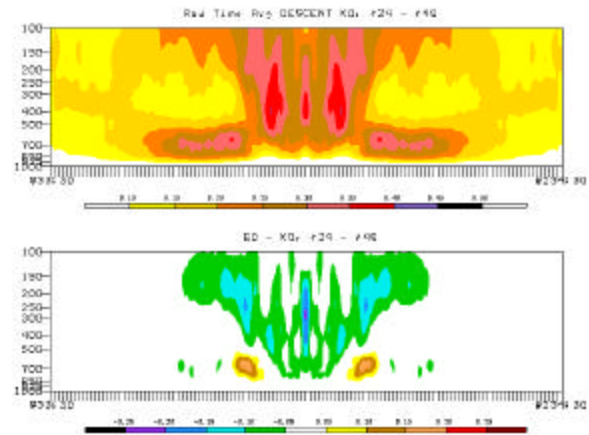


Fig. 7. As above for K0 (top), and the difference field (bottom) with K0 subtracted from B0.

### 5.5 Temperature Structure

The temperature structure of all simulations is evaluated by comparing  $\theta$  fields. A tri-pole feature is apparent when comparing both the B0 and BB cases as well as the K0 and KK runs, although this pattern is of a smaller magnitude in the KF runs (Fig. 8).

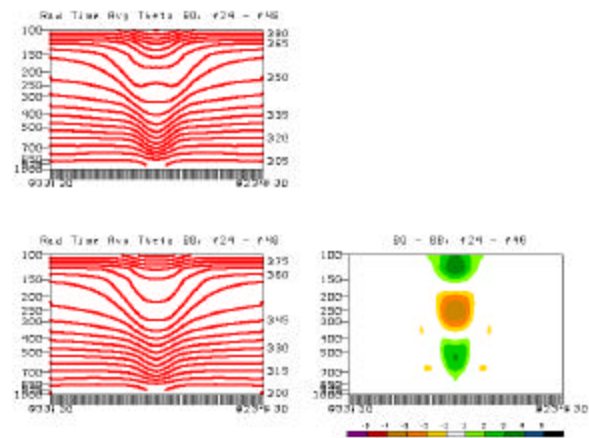


Fig. 8. Radial and time averaged cross-sections of  $\theta$  plotted every  $15^\circ \text{ K}$  for B0 (top left), BB (bottom left). The difference field (bottom right) with BB subtracted from B0 is shaded every  $1^\circ \text{ K}$ . Here, warmer colors are shaded where BB is greater than B0, while cooler shading is used where B0 is greater.

The B0 case does produce a warmer core at lower levels, but an area of cooler temperatures in the B0 simulation is located above. At the upper levels of the eye, the explicit run again shows warmer temperatures than in the CP simulation.

## 6. CONCLUSIONS AND FUTURE WORK

As expected, the use or omission of a CP scheme in these simulations did result in significant differences in the intensity, vertical motions, and thermodynamic structure of Hurricane Ivan. Comparisons between the B0 and BB cases show similar trends as when K0 and KK are juxtaposed, indicating that the results are not specific to an individual scheme but are representative of the effects of using CP schemes versus explicitly resolved convection. Explicit convection on the 3 km finer-mesh grid generally results in a deeper tropical cyclone with stronger vertical motions and a warmer low-level core.

The explicit treatment of convection results in grid-scale instability and vertical motion, making these vertical motions stronger since there is no subgrid-scale parameterization to remove instability. Consistent with the discussion of Ooyama (1982), explicit convection allows the model to resolve the storm's secondary circulation directly. Stronger eyewall ascent gives rise to strengthened compensating subsidence. Adiabatic warming from increased subsidence produces a warmer core, thereby contributing to a hydrostatic reduction of the cyclone central pressure and increased convergence of the surface winds, which leads to stronger turbulent fluxes and a more intense hurricane (Emanuel 1986).

The differences between CP and explicit runs are generally of lesser magnitude in contrasting the two KF simulations (K0 and KK) than when an analogous comparison is made between the two BMJ cases (B0 and BB). With KF being a mass-flux scheme and BMJ an adjustment scheme, KK looks more similar to K0 than BB does to its counterpart explicit simulation. However, the B0 case did produce an 18 hPa deeper hurricane than the K0 simulation. Therefore, these results do support previous work that showed that the use of different CP schemes on the outer grids can significantly impact convection resolved on the inner grid (e.g., Warner and Hsu 2000).

Future work will involve additional in-depth analysis of these simulations as well as observational comparisons. Additional research questions include the physical origin of the tri-pole feature seen in the  $\theta$  difference fields between the two KF and the two BMJ runs. As mentioned above, points farther away from the storm are better sampled than the points closer to the center, so signals seen closer to the storm center are less reliable in the radial averaged variables than those farther away. However, this colder mid-level core in the explicit cases is also seen in the original data before averaging.

Additional future work will include investigating the effects of further decreasing the horizontal grid spacing to determine the coarsest resolution that can produce realistic convection without parameterization in a tropical cyclone.

## 7. ACKNOWLEDGEMENTS

This research was supported by NSF grant ATM-0334427, awarded to North Carolina State University. The WRF model was made available through NCAR, sponsored by the NSF. GFS initial conditions were provided by NCDC, and SST data were provided by NCEP. The authors would like to acknowledge the current and former members of the Meteorological Analysis and Prediction Laboratory at North Carolina State University, including Dr. Michael Brennan, Kelly Mahoney, and Kevin Hill, who made themselves available to answer the many modeling questions and problems raised to the 1<sup>st</sup> author during this research effort.

## 8. REFERENCES

- Betts, A. K., and M. J. Miller, 1993: The Betts–Miller scheme. *The Representation of Cumulus Convection in Numerical Models, Meteor. Monogr.*, No. 46, Amer. Meteor. Soc., 107–122.
- Bryan, G. H., J. C. Wyngaard, and J. M. Fritsch, 2003: Resolution requirements for the simulation of deep moist convection. *Mon. Wea. Rev.*, **131**, 2394–2416.

Davis, C., and L. F. Bosart, 2002: Numerical simulations of the genesis of Hurricane Diana (1984). Part II: Sensitivity of track and intensity prediction. *Mon. Wea. Rev.*, **130**, 1100–1124.

Emanuel, K. A., 1986: An air-sea interaction theory for tropical cyclones. Part I: Steady state maintenance. *J. Atmos. Sci.*, **43**, 585–604.

Janjic, Z. I., 1994: The step-mountain Eta coordinate model: Further development of the convection, viscous sublayer and turbulent closure schemes. *Mon. Wea. Rev.*, **122**, 927–945.

Kain, J. S., and J. M. Fritsch, 1993: Convective parameterization for mesoscale models: The Kain–Fritsch scheme. *Cumulus Parameterization, Meteor. Monogr.*, No. 46, Amer. Meteor. Soc., 165–170.

Ooyama, K. V., 1982: Conceptual evolution of the theory and modeling of the tropical cyclone. *J. Roy. Meteor. Soc. Japan*, **60**, 369–379.

Stewart, S. R., cited 2006: National Hurricane Center Tropical Cyclone Report: Hurricane Ivan. [Available from <http://www.nhc.noaa.gov/2004ivan.shtml>]

Thiébaux, J, E Rogers, W Wang, and B Katz, 2003: A new high-resolution blended real-time global sea surface temperature analysis. *Bull. Amer. Meteor. Soc.*, **84**, 645–656

Warner, T. T., and H. M. Hsu, 2000: Nested-model simulation of moist convection: The impact of course-grid parameterized convection on fine-grid resolved convection. *Mon. Wea. Rev.*, **128**, 2211–2231.

Weisman, M. L., W. C. Skamarock, and J. B. Klemp, 1997: The resolution dependence of explicitly modeled convective systems. *Mon. Wea. Rev.*, **125**, 527–548.